

FTS Measurements of Submillimeter-Wave Atmospheric Opacity at Pampa la Bola

III. Water Vapor, Liquid Water, and 183 GHz Water Vapor Line Opacities

Satoki MATSUSHITA

Harvard-Smithsonian Center for Astrophysics, 60 Garden Street, MS-78, Cambridge, MA 02138, USA
smatsushita@cfa.harvard.edu

and

Hiroshi MATSUO

Advanced Technology Center, National Astronomical Observatory of Japan, Mitaka, Tokyo 181-8588
h.matsuo@nao.ac.jp

(Received 2002 August 12; accepted 2002 November 16)

Abstract

Further analysis has been made on the millimeter and submillimeter-wave (100–1600 GHz or 3 mm – 188 μm) atmospheric opacity data taken with the Fourier Transform Spectrometer (FTS) at Pampa la Bola, 4800 m above sea level in northern Chile, which is the site of the Atacama Large Millimeter/submillimeter Array (ALMA). Time-sequence plots of millimeter and submillimeter-wave opacities show similar variations to each other, except for during the periods with liquid water (fog or clouds) in the atmosphere. Using millimeter and submillimeter-wave opacity correlations under two conditions, which are affected and not affected by liquid water, we succeeded to separate the measured opacity into water vapor and liquid water opacity components. The water vapor opacity shows good correlation with the 183 GHz water vapor line opacity, which is also covered in the measured spectra. On the other hand, the liquid water opacity and the 183 GHz line opacity show no correlation. Since only the water vapor component is expected to affect the phase of interferometers significantly, and the submillimeter-wave opacity is less affected by the liquid water component, it may be possible to use the submillimeter-wave opacity for a phase-correction of submillimeter interferometers.

Key words: atmospheric effects — instrumentation: spectrometer — site testing — submillimeter

1. Introduction

In astronomy, observations with millimeter and submillimeter wavelengths are highly suitable for studying molecular gas and dust emission from various astronomical objects, including young stellar objects, star-forming/starburst regions, and primeval galaxies. However, observations at these frequencies/wavelengths, especially at submillimeter-wavelength, are difficult, since it is easily and heavily absorbed by water constituents in the atmosphere. Therefore, understanding the absorption/emission spectra caused by the water constituents is important, but is not yet well characterized.

At the high-altitude site of the Atacama desert in Northern Chile (Pampa la Bola – Chajnantor region, about 5000 m above the sea level), the US, Europe, and Japan are planning to build the Atacama Large Millimeter/submillimeter Array (ALMA), which will be the world's largest millimeter and submillimeter interferometer. Since the site is very dry, it is a suitable location for studying the behavior of water constituents in the millimeter/submillimeter region. At Pampa la Bola – Chajnantor area, 220 GHz/225 GHz tipping radiometers (Kohno et al. 1995; Radford, Holdaway 1998; Radford,

Chamberlin 2000; Radford et al. 2001; Radford 2002; Sakamoto 2002), a 350 μm tipping photometer (Radford, Holdaway 1998; Radford 2002), 183 GHz water line radiometers (Delgado et al. 1999, 2000, 2001), and 11 GHz radio seeing monitors (Radford et al. 1996; Holdaway et al. 1997; Radford, Holdaway 1998; Butler et al. 2001; Radford 2002; Sakamoto 2002) are now continuously operating to evaluate the absorption and phase fluctuation caused by water constituents. Also, a 492 GHz tipping radiometer performed measurements for intermittent periods of time (Hirota et al. 1998). We then carried out wide frequency coverage opacity measurements using a Fourier Transform Spectrometer (FTS) in the winter of 1997 and 1998.

Opacity measurements with the FTS were performed during 1997 September 5 and 12. Opacity correlations between 220 GHz and all the submillimeter-wave windows were obtained, although the weather conditions were limited (Matsuo et al. 1998a,b). During 1998 June 16 and 18, opacities under good weather conditions were measured, and high transmission spectra as well as the detection of supra-terahertz windows located around 1035 GHz, 1350 GHz, and 1500 GHz have been obtained (Matsushita et al. 1999, 2000; Matsushita, Matsuo 2002). These

supra-terahertz windows have also been detected by other groups (Paine et al. 2000; Pardo et al. 2001b, 2002) and successfully modeled with radiative transfer calculations (Pardo et al. 2001a,b, 2002; Matsushita et al. 1999, 2000). Combining these data sets with long-term site testing radiometer data (Radford, Holdaway 1998), the fraction of time with a low-opacity condition in submillimeter-wave (675 GHz and 875 GHz) atmospheric windows at the ALMA site was estimated. The submillimeter zenith opacity is less than 1.0 for about 50% of the winter season and about 37% of a year, which is about 50% better than the Mauna Kea site (Matsushita et al. 1999).

During the measurement period in 1998, quite different opacity correlations compared with the normal ones mentioned above were obtained. Because of their behavior, weather condition, and theoretical perspectives, it is suggested that liquid water in the atmosphere caused these correlation changes (Matsushita et al. 1999; Matsushita, Matsuo 2002). We analyzed these ‘abnormal’ opacity correlation data in detail, and considered the effect of liquid water on millimeter- and submillimeter-waves. Based on these results, we propose new phase-correction methods for submillimeter interferometry.

2. Measurements and Data Analysis

Atmospheric opacity measurements were performed at Pampa la Bola (northern Chile, the Atacama desert, 4800 m altitude) using a Martin-Puplett type FTS (Martin, Puplett 1970) and an InSb bolometer. The frequency coverage was 100–1600 GHz (or 3 mm to 188 μm in the wavelength range). Two different observing runs were carried out, the first one in 1997 September 5–12, and the second one in 1998 June 16–18 (both in winter season in Chile).

The beam size of the instrument was about 10° , and the apodized frequency resolution was $\sim 0.3 \text{ cm}^{-1}$ ($\sim 10 \text{ GHz}$). Atmospheric emission spectra were obtained toward different air masses [$\sec(z)$, z is zenith angle] at 1.0, 1.5, 2.0, 2.5, and 3.0 by rotating a tipping mirror outside of the spectrometer. A tipping measurement with the FTS including two temperature calibrations was made every 12 min in the first observing run and every 14 min in the second run. The absolute-brightness temperature of the atmosphere was calibrated using blackbodies (Eccosorb AN74) at liquid-nitrogen temperature ($\sim 73 \text{ K}$ at 4800 m altitude) and at ambient temperature. The ambient temperature was monitored with a weather station (Sakamoto et al. 2000). In data analysis, tipping measurements were used for frequencies lower than 450 GHz, and temperature measurements were used for frequencies higher than 450 GHz. From 10 PM on June 17 to 4 AM on June 18 in 1998, however, temperature measurements were used for all frequencies. This is because the existence of clouds in the atmosphere is suggested (see subsection 4.1), and therefore requirements for tipping measurement (need a constant sky condition toward different air masses and a low opacity condition) would not be satisfied. Further details on the instruments, measurements, calibrations,

and data analysis are described elsewhere (Matsuo et al. 1998a,b; Matsushita et al. 1999).

Since the frequency coverage of our FTS data ranges from 100 GHz, we can measure the 183 GHz water vapor line opacity by subtracting the continuum component from both sides of the line. We assumed 161–204 GHz as the 183 GHz water vapor line frequency range, and 136–161 GHz and 204–230 GHz as continuum frequency ranges. The continuum opacity within the line frequency range was calculated with the interpolation of the continuum opacities located at both sides of the line. After continuum subtraction, the line opacity was divided by the number of the data points within the line frequency range (12 points), since our FTS frequency resolution is not good enough to resolve the 183 GHz line. The 183 GHz opacity used in this paper is, therefore, the average opacity in this frequency range.

3. Time-Variations of Measured Opacities

Time-variation plots for 220, 345, 492, 675, 875, and 937 GHz opacities are shown in figure 1. The selected frequencies are either located at the center of atmospheric windows and/or are frequencies of special astronomical interests (see Matsushita et al. 1999; Matsushita, Matsuo 2002). The left-hand and right-hand sides of the figure are the data taken in 1997 and 1998, respectively. In the 1997 measurement, because the sensitivity of the bolometer in daytime data had large variations, we only used nighttime data.

The time-variation plots of the 1997 data (the left-hand side of figure 1) clearly show that the opacity condition was relatively good at the beginning of the measurement (1997 September 5), but gradually worsened toward the end (1997 September 12). The overall time variations of the plots look similar to each other, except for the plot of 937 GHz which saturates under worse weather conditions.

On the other hand, the time-variation plots of the 1998 data (the right-hand side of figure 1) indicate that the opacity condition was extremely good during the first half of the measurement (from the evening of June 16 to around noon of 17), but gradually worsened from the afternoon of June 17, and became totally bad around midnight. The lowest opacity (the best atmospheric transmission; see figure 1 in Matsushita et al. 1999) was recorded around noon on June 17 (Chilean local day of around 17.5 in the plots). The first half of the time-variation plots looks similar for all frequencies (from 220 GHz to 937 GHz), but the second half, especially around the beginning of June 18, of the plots is different between the lower frequencies (220 GHz and 345 GHz) and higher frequencies. The implications of this is discussed in a later section.

Figure 2 shows time-variation plots of the supra-terahertz windows. Since the weather condition of the 1997 measurement was not good enough to detect these supra-terahertz windows, we only show the 1998 data. Because the sensitivity of our FTS around the 1350 GHz and 1500 GHz windows is low and has some systematic

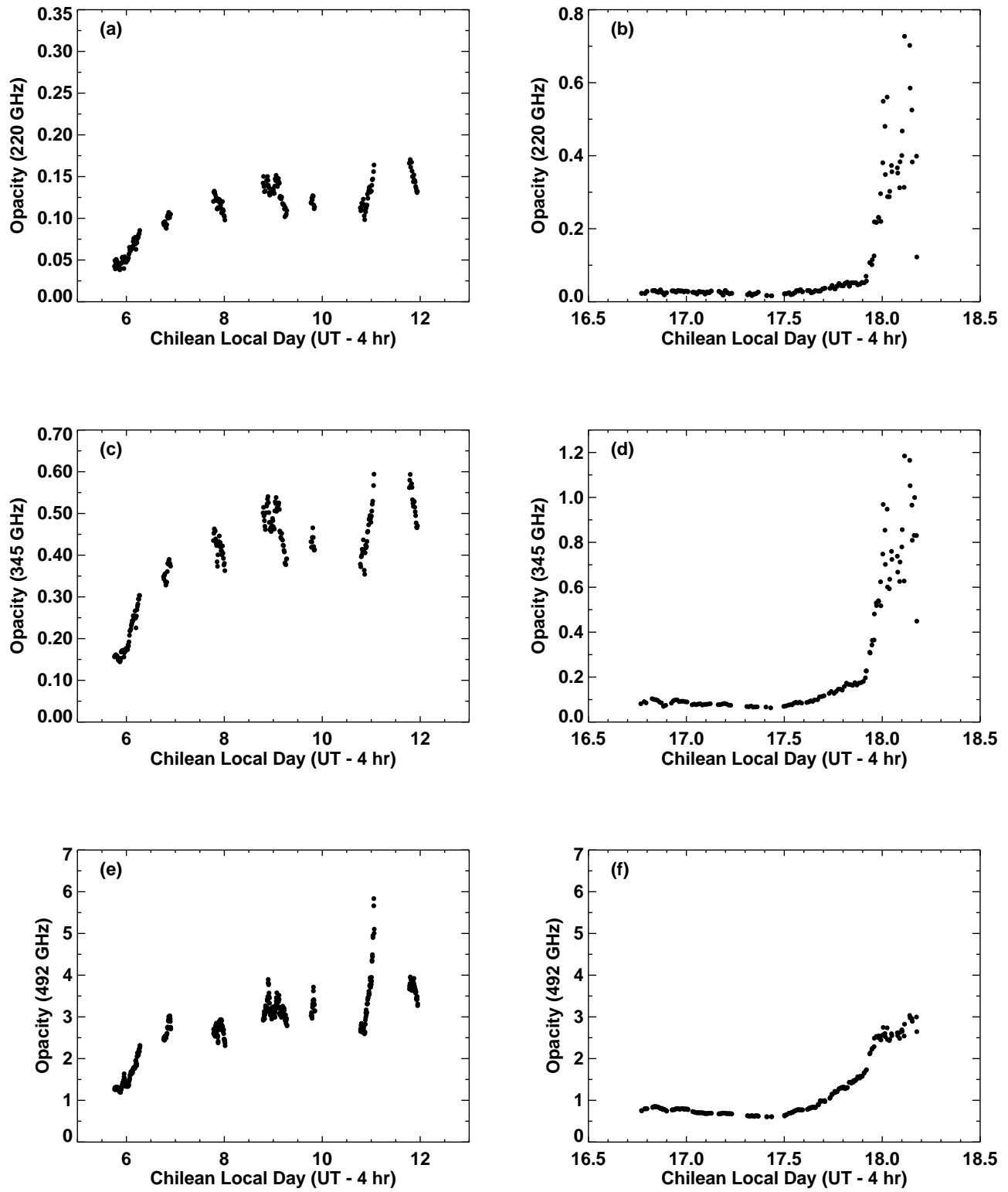


Fig. 1. Time-sequence plots for 220, 345, 492, 675, 875, and 937 GHz opacities. The left-hand and right-hand sides of the figure are the data taken in 1997 September and 1998 June, respectively. The Chilean local time corresponds to $UT - 4$ hr.

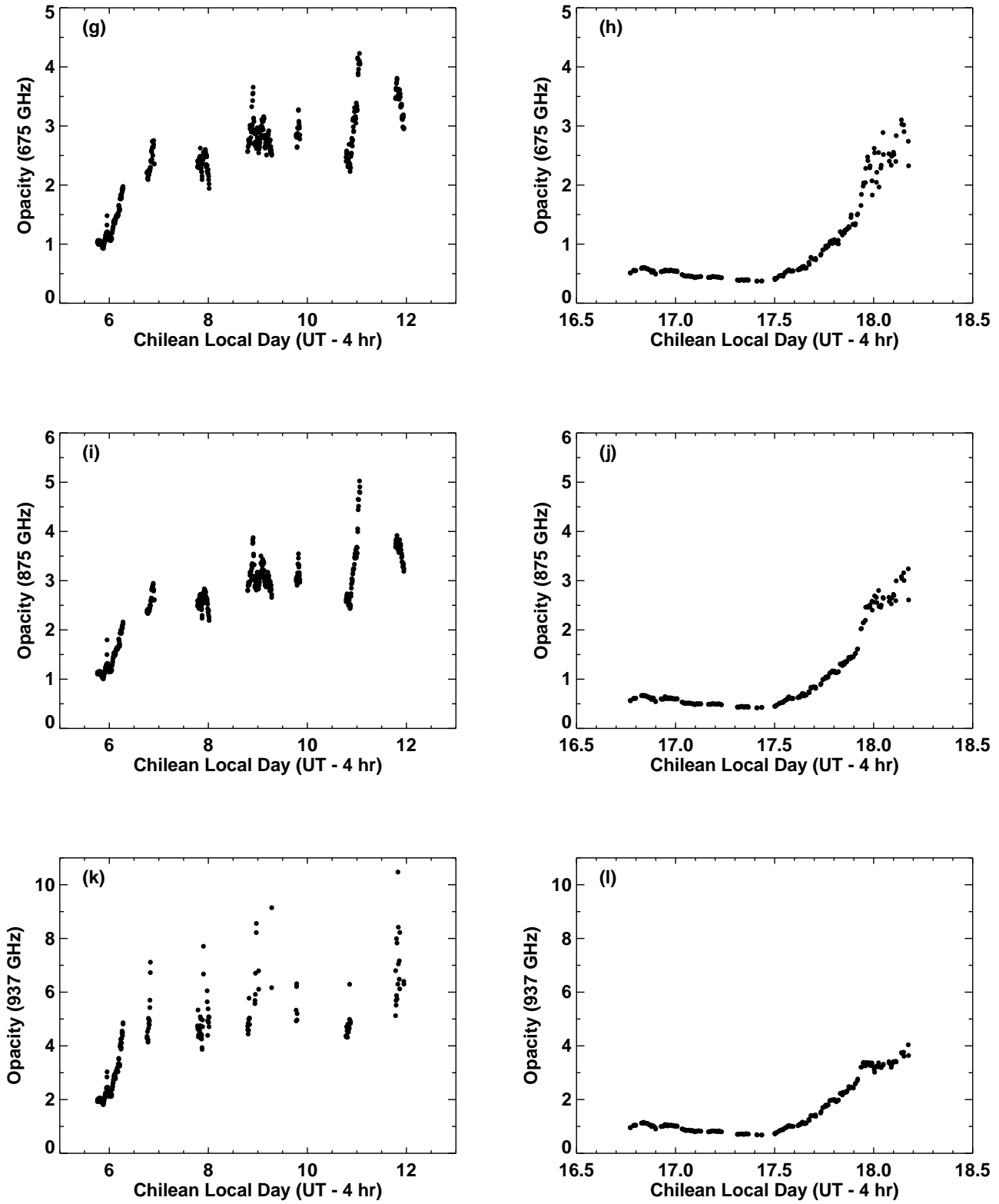


Fig. 1. (Continued)

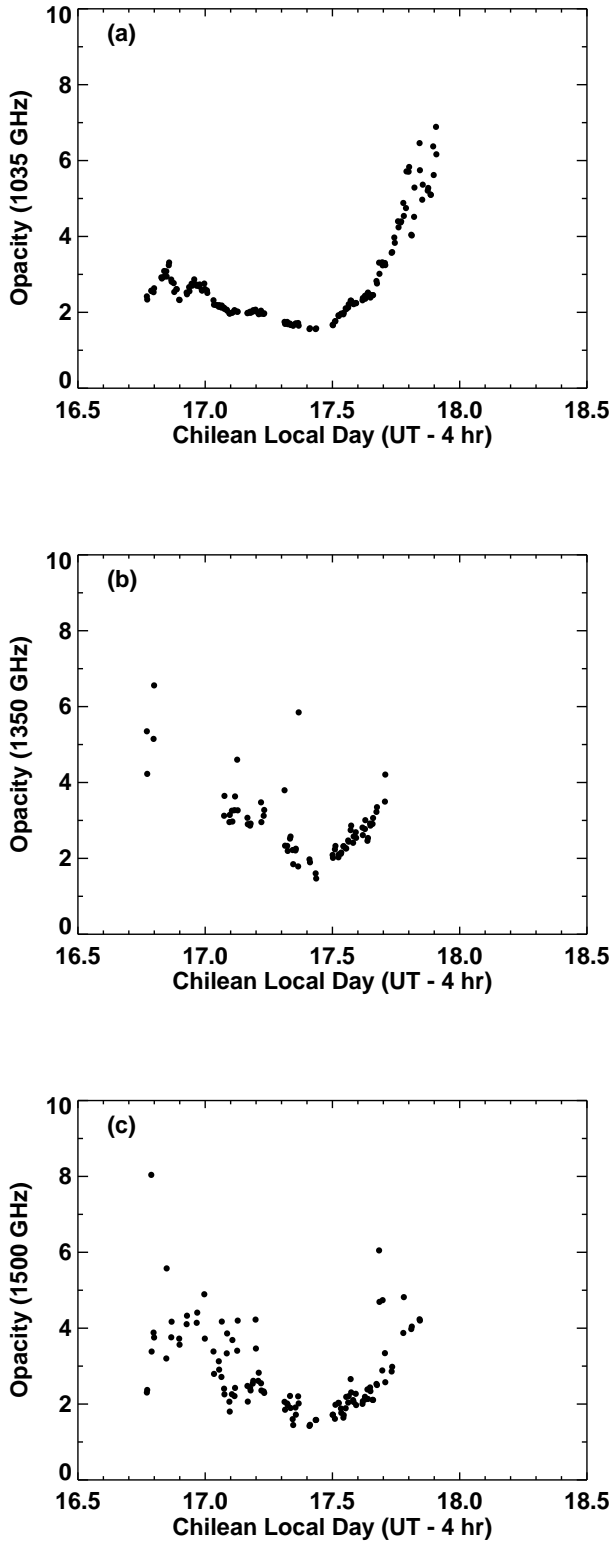


Fig. 2. Time-sequence plots for (a) 1035 GHz, (b) 1350 GHz, and (c) 1500 GHz opacities. The Chilean local time corresponds to $UT - 4$ hr. Since the weather conditions during the 1997 measurement were not good enough to detect these supra-terahertz windows, we only show 1998 data plots.

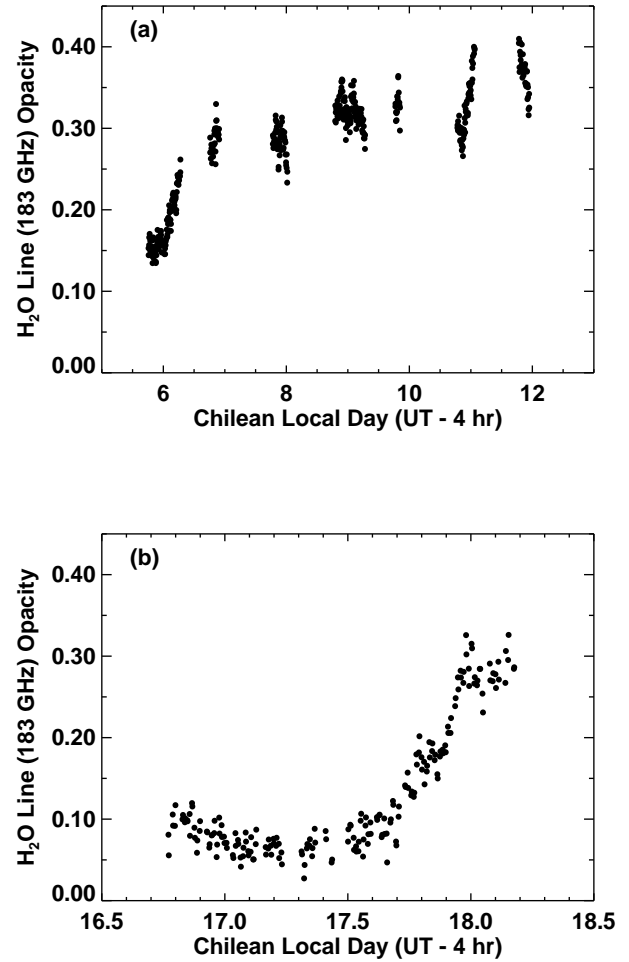


Fig. 3. Time-sequence plots for 183 GHz water vapor line opacity averaged over 161 to 204 GHz, taken in (a) 1997 September and (b) 1998 June. The Chilean local time corresponds to $UT - 4$ hr.

errors (see Matsushita et al. 1999 for detail), the plots have a larger scatter than the other plots. Still, the plots show a similar trend to the others.

We also plot the time variation of the 183 GHz water vapor line opacity (figure 3). The 1997 data plot (figure 3a) shows similarities to the other opacity plots (the left-hand side of figure 1). The 1998 data plot (figure 3b) shows similar variation to the higher frequency (≥ 492 GHz) plots (the right-hand side of figure 1 and figure 2), but different from the lower frequency (220 GHz and 345 GHz) plots, especially from the late evening of June 17 to the early morning of June 18.

4. Analysis of Water Vapor and Liquid Water Opacity Components

4.1. 'Abnormal' Opacity Correlations between Millimeter- and Submillimeter-Wave

Usually, correlation plots between 220 GHz opacity and submillimeter window opacities are strongly correlated with coefficients of 22–24 (hereafter we refer to these cor-

relations as ‘normal’ correlations; Matsuo et al. 1998a; Matsushita et al. 1999, 2000; see also Masson 1994). However, from 17.9 to 18.2 Chilean local day (from 10 PM on June 17 to 4 AM on June 18) in 1998, we obtained quite different correlation plots from the ‘normal’ correlations (see figure 4 in Matsushita et al. 1999). These ‘abnormal’ plots show lower correlation coefficients and larger zero-point offsets than those of the ‘normal’ correlations, which means that the fractional variation of the millimeter opacity is much larger than the submillimeter opacity.

The NRAO surveillance camera at the Chajnantor site (<http://www.tuc.nrao.edu/alma/site/site.html>) shows a clear sky image around 5 PM on June 17, but shows a cloudy image around 9 AM on June 18. In addition, the ambient temperature data taken by the weather station (Sakamoto et al. 2000) recorded temperature below freezing (around -5°C to -8°C). These weather data suggest that there were water droplets (liquid water), or ice particles, in the atmosphere when we obtained the ‘abnormal’ correlation data.

Water vapor absorbs stronger in the submillimeter-wave region than in the millimeter-wave region (Liebe 1989; Liebe et al. 1993; Pardo et al. 2001a). Liquid water (cloud or fog), on the other hand, absorbs more effectively at the millimeter-wave region for a given particle-size distribution (Ray 1972; Liebe 1989; Liebe et al. 1991; see also Matsushita et al. 2002), which means that a variation in the quantity of the liquid water content in the atmosphere causes a large change in the millimeter-wave opacity. The existence of ice cannot explain the ‘abnormal’ correlations. Ice has about two orders of magnitude lower values for the imaginary part of the index of refraction (\approx absorption coefficient¹) at millimeter-wave region than that of liquid water (Warren 1984; Liebe et al. 1993; Hufford 1991; Ray 1972), and is similar to that of water vapor.

There is a possibility that other molecules or aerosols cause the ‘abnormal’ correlations. Neither the oxygen nor ozone lines can be the cause, since these show up with narrow lines in the spectra (e.g., Pardo et al. 2001a; Matsushita et al. 1999). The characteristics of the wet and dry pseudocontinuum components, which are thought to be the far wings of water vapor lines in the infrared range and collision-induced absorption of the dry atmosphere (N_2 and O_2), respectively (Pardo et al. 2001a,b, 2002), are still empirical and not well understood. Furthermore, the wet pseudocontinuum should be correlated with water vapor, and the dry atmosphere should have a constant density and is not expected to fluctuate. In addition, since the wet and dry pseudocontinuum absorptions at millimeter-wave are too weak to explain the ‘abnormal’ correlations, we have to introduce a new kind of pseudocontinuum absorption component, which has rather stronger absorption in the millimeter-wave range than the other pseudocontinuum components. However, it is beyond the scope of our paper to introduce the new pseudocontinuum component.

¹ The imaginary part of the complex index of refraction, n_I , and the absorption coefficient, α , is related as $\alpha = 4\pi\nu n_I/c$ (Thompson et al. 2001).

Table 1. Correlation coefficients of the ‘normal’ (a_{WV}) and ‘abnormal’ (a_{LQ}) correlations between 220 GHz opacity and submillimeter opacities.

Frequency (GHz)	a_{WV}^*	a_{LQ}
345	3.65 ± 0.02	1.42 ± 0.03
410	7.53 ± 0.05	1.64 ± 0.05
492	23.6 ± 0.3	1.5 ± 0.2
675	22.4 ± 0.2	1.9 ± 0.2
875	24.2 ± 0.2	1.8 ± 0.2
937	43.9 ± 0.9	0.6 ± 0.2

* The values are taken from Matsushita et al. (2000).

We therefore suggest that the ‘abnormal’ correlations are caused by the effect of the liquid water absorption, which is the most plausible known component. The reason why liquid water still existed in the atmosphere even when the ambient temperature was below freezing may be that the atmospheric temperature at the clouds was warmer than that on the ground, or that the clouds consisted of both liquid water and ice, but the absorption caused by liquid water dominated the total atmospheric absorption.

4.2. Separation of Total Opacity into Two Opacity Components

To confirm this suggestion, we separate the total opacity into water vapor opacity and liquid water opacity components using the ‘normal’ and ‘abnormal’ correlations between millimeter and submillimeter opacities. For the separation, we assume that (a) the ‘normal’ correlations result only from the water vapor absorption, (b) ‘abnormal’ correlations are the combined effect of the water vapor and liquid water absorptions, (c) the correlation coefficients of the liquid water absorption correspond to those of the ‘abnormal’ correlations, and (d) the zero-point offsets are zero in all the correlations. Under these assumptions, we can write:

$$\tau_{\nu,\text{WV}} = a_{\text{WV}} \cdot \tau_{220,\text{WV}}, \quad (1)$$

$$\tau_{\nu,\text{LQ}} = a_{\text{LQ}} \cdot \tau_{220,\text{LQ}}, \quad (2)$$

$$\tau_{220} = \tau_{220,\text{WV}} + \tau_{220,\text{LQ}}, \quad (3)$$

$$\tau_{\nu} = \tau_{\nu,\text{WV}} + \tau_{\nu,\text{LQ}}, \quad (4)$$

where τ_{220} and τ_{ν} indicate opacities at 220 GHz and frequency ν , and the suffix WV and LQ indicate water vapor and liquid water components, respectively. The known (measured) parameters are a_{WV} , a_{LQ} , τ_{220} , and τ_{ν} . Using these parameters, we can separate the water vapor and liquid water opacity components from the measured total opacity. We summarized the a_{WV} and a_{LQ} of the selected frequencies derived from the ‘normal’ (Matsushita et al. 2000) and ‘abnormal’ (Matsushita et al. 1999) correlations in table 1.

We then performed the component separation on the 220 GHz and 675 GHz opacities taken in 1998, and the results of the separated millimeter and submillimeter opacities are shown in figure 4. The top row of figure 4 shows

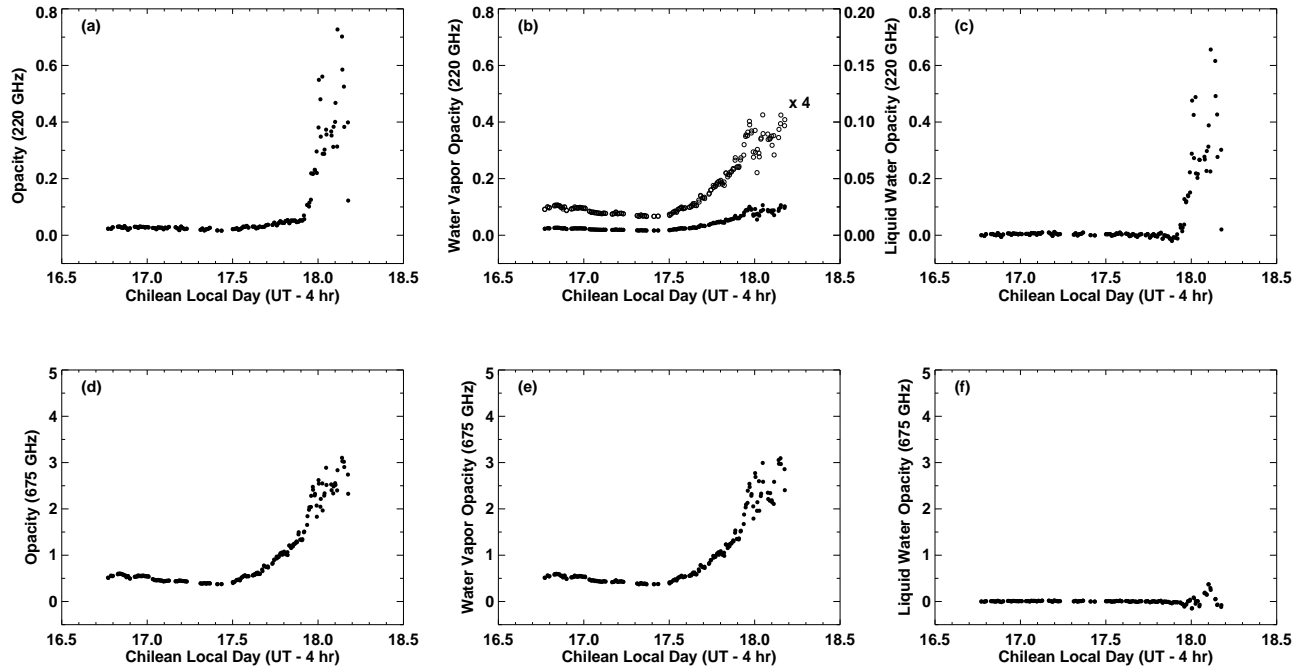


Fig. 4. Time variations of (a) total 220 GHz opacity, (b) 220 GHz separated water vapor opacity (filled circles, see left-hand axis for their unit), overplotted with the same plot but multiplied by four (open circles, see right-hand axis), (c) 220 GHz separated liquid water opacity, (d) total 675 GHz opacity, (e) 675 GHz separated water vapor opacity, and (f) 675 GHz separated liquid water opacity. The data were taken during the 1998 measurement, and the Chilean local time corresponds to UT $-$ 4 hr.

the time variations at 220 GHz for (a) the total opacity, (b) the separated water vapor opacity, and (c) the separated liquid water opacity. The bottom row shows the same plots but for 675 GHz. The total opacity plots for 220 GHz and 675 GHz (figures 4a,d) look different, especially around Chilean local day from 17.9 to 18.2, but the separated water vapor opacity plots (figures 4b,e) show similar time variation to each other. On the other hand, the 220 GHz separated liquid water opacity plot (figure 4c) shows a quite different behavior from that of 675 GHz (figure 4f), when the ‘abnormal’ correlation occurred. These results suggest that millimeter opacity is largely affected by the liquid water component in the atmosphere, although the effect in submillimeter opacity is small.

4.3. Correlations with 183 GHz Water Vapor Line Opacity

To further confirm that the separated water vapor and liquid water opacities were really caused by these components in the atmosphere, it is very important to compare these with the 183 GHz water vapor line opacity. To this end, we made correlation diagrams between the 183 GHz line opacity and those of total, water vapor, and liquid water at 220 GHz (millimeter) and 675 GHz (submillimeter), as shown in figure 5. The correlation diagram between the 183 GHz line opacity and 220 GHz total opacity (figure 5a) shows a large scatter, but after the separation, the 220 GHz water vapor opacity shows good correlation with the 183 GHz line opacity (figure 5b). On the other hand, the 220 GHz liquid water opacity is completely indepen-

dent from the 183 GHz line opacity (figure 5c). These results confirm the success of the opacity component separation.

The correlation diagram of the 183 GHz line opacity and the 675 GHz total opacity (figure 5d) is similar to that of the 183 GHz line opacity and the 675 GHz water vapor opacity. The correlation diagram of the 183 GHz line opacity and the 675 GHz liquid water opacity, on the other hand, shows little contribution of liquid water in the 675 GHz opacity. These results support that the submillimeter opacity is dominated by water vapor absorption, and less affected by liquid water absorption.

The correlation diagrams between the water vapor opacity and the 183 GHz line opacity (figures 5b,e) show a somewhat curved structure. The curve at the lower end of the opacity, which shows an offset from the zero opacity of the water vapor opacity, is caused by the limitation of the measurements (see Matsuo et al. 1998a,b) and/or by both the wet and dry pseudocontinuum absorptions. The curve at the upper end can be explained by the saturation of the 183 GHz line. This saturation is theoretically expected (Lay 1998; Carilli et al. 1998) and also observed with multi-channel 183 GHz line radiometers (Wiedner, Hills 2000; Yun, Wiedner 1999; Wiedner et al. 2001).

5. Application for Phase-Correction

The most unwanted atmospheric effect for millimeter/submillimeter interferometers is excess paths in electromagnetic wave propagations caused by water vapor. A fluctuation in the path difference between a pair of anten-

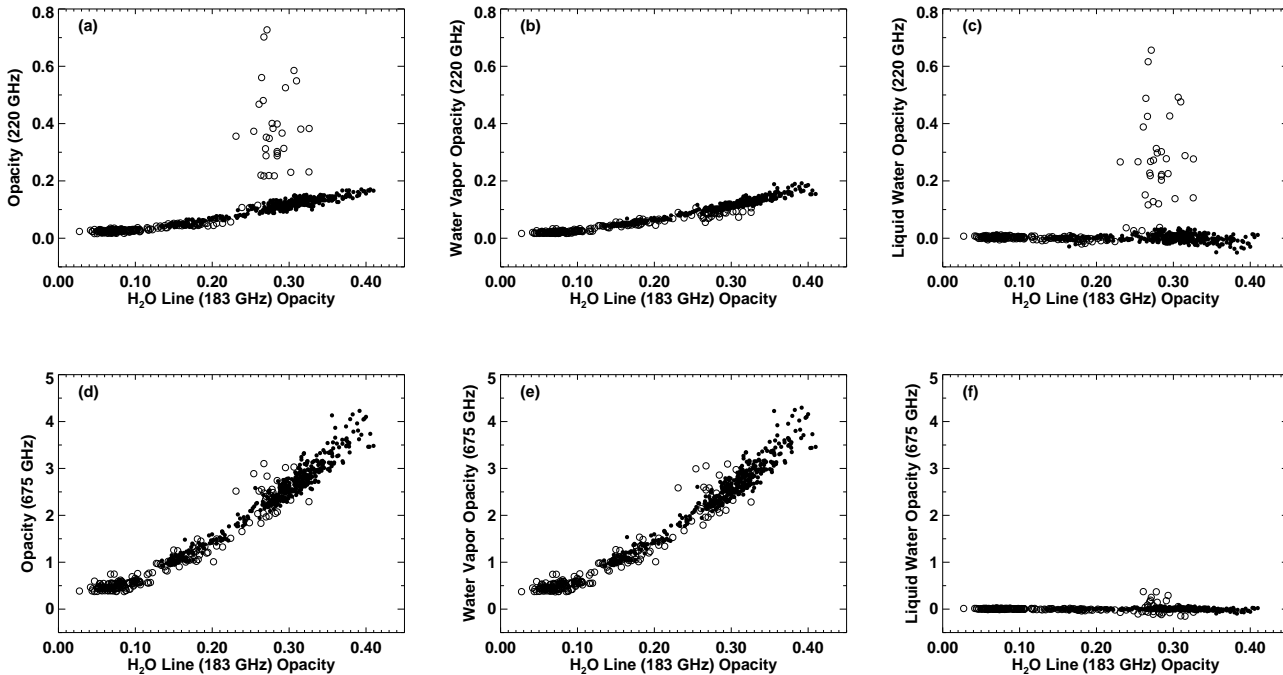


Fig. 5. Correlation diagrams between 183 GHz water-vapor line opacity averaged over 161 to 204 GHz and (a) total 220 GHz opacity, (b) 220 GHz separated water vapor opacity, (c) 220 GHz separated liquid water opacity, (d) total 675 GHz opacity, (e) 675 GHz separated water vapor opacity, and (f) 675 GHz separated liquid water opacity. The filled and open circles indicate the dataset taken in 1997 September and 1998 June, respectively.

nas causes phase fluctuation, which decreases the interferometric data quality noticeably. Since the characteristics of water vapor are theoretically and observationally well known, it is better to use its absorption for phase-correction methods. Liquid water, on the other hand, has a different index of refraction from that of water vapor (Thompson et al. 2001; Ray 1972; Liebe 1989), and its contribution to the opacity at lower frequency is much higher than that of water vapor, but affects the phase fluctuations less (Matsushita et al. 2002). In addition, the characteristics of liquid water are poorly understood. Hence, for phase-corrections using opacity (brightness temperature) of the atmosphere, one should measure the *water vapor* opacity instead of the opacity affected by *liquid water*.

Based on the results and discussion in the previous section, we suggest that an accurate phase-correction for interferometers can be made using (a) 183 GHz water vapor line radiometers, which avoids the line center that can be easily saturated, (b) submillimeter-wave radiometers whose frequency range is much less affected by the liquid water absorption, or (c) two frequency (millimeter- and submillimeter-wave) radiometers which can separate the water vapor and liquid water components, as mentioned above.

The phase-correction method (a) has already been discussed and demonstrated by many authors (Wiedner et al. 2001, 2002; Delgado et al. 2001; Wiedner, Hills 2000).

Method (b) needs either one radiometer in each antenna, or it is also possible to use the total power output from a submillimeter receiver for astronomical observa-

tions, and hence no additional instruments are required. Although the effect of liquid water in the submillimeter-wave is much less than that in millimeter-wave, this method may be inaccurate under a large liquid water content. We can estimate the phase-correction errors due to the liquid water content, assuming that it contributes to a typical 220 GHz opacity scatter of 10%. The estimated errors are 19 μm , 42 μm , and 71 μm under 220 GHz opacities (τ_{220}) of 0.016 (the best condition at the ALMA site; Matsushita et al. 1999), 0.036, and 0.061 (25% and 50% quartile of τ_{220} , respectively; Radford, Chamberlin 2000), respectively. These errors correspond to phase errors of 15°, 34°, and 57° at 675 GHz, respectively, which are the accuracies for this phase-correction method (see Matsushita et al. 2002 for detail).

Method (c) needs two radiometers in each antenna or uses the total power outputs of both millimeter and submillimeter receivers that operate simultaneously. In spite of the system complexity, this method is advantageous, since there are fewer errors due to the liquid water content. One important question is whether a_{LQ} is constant or not. The emission properties of liquid water as a function of frequency will depend on droplet size and temperature, which are likely to change from night to night. More measurements under large liquid water content are needed. However, the general trend, i.e., submillimeter measurements are less affected by liquid water, does not change. If the uncertainty of the liquid water model is 10%, the error of the 675 GHz total power phase-correction mentioned above will be reduced by 1/10 (Matsushita et al. 2002).

The merit of method (b) is that the field of view for

the phase-correction is exactly the same as that of the astronomical observations. A disadvantage of submillimeter phase-correction methods is that they cannot be used to observe in submillimeter-wavelength under bad weather conditions, and therefore cannot be applied to a site where the submillimeter opacity is large.

On the other hand, in some cases, the effect of ice particles might exist. Since the absorption characteristics of ice particles are similar to those of water vapor (see subsection 4.1), it may be difficult to distinguish between these two absorptions by the methods (b) and (c). In addition, it is not clear to which amount of ice particles usually exist in the atmosphere. These might be one of the uncertainties in the proposed total-power phase-correction methods. To clarify these problems, further measurements of atmospheric opacity spectra due to ice particles and detailed theoretical modelings will be needed.

To check the feasibility of the newly proposed methods (b) and (c), test measurements with other phase-correction methods, such as the method (a), or the fast-switching method (Holdaway 1992; Holdaway, Owen 1995; Carilli et al. 1996; Carilli, Holdaway 1997, 1999; Morita et al. 2000) should be performed. The best available instrument for such tests is the Sub-Millimeter Array (SMA; Ho 2000) on Mauna Kea, Hawaii, which is being constructed by the Smithsonian Astrophysical Observatory (SAO) and the Academia Sinica Institute of Astronomy and Astrophysics (ASIAA) of Taiwan. SMA has a similar observing frequency range to ALMA (180–900 GHz), and will have a capability of dual-frequency operation. In addition, two 183 GHz radiometers (Wiedner et al. 2001) are already installed, and improved 183 GHz radiometers (Hills et al. 2001) are being developed. SMA will therefore be an ideal instrument to evaluate the proposed total-power phase-correction methods and other various methods.

6. Conclusion

We have made further analyses on the FTS measurements of millimeter and submillimeter atmospheric opacity taken at Pampa la Bola. Part of the 1998 opacity data is heavily affected by liquid water in the atmosphere, which served to understand the absorption spectrum of liquid water. We successfully separated the measured opacity into water vapor and liquid water opacity components. The separated water vapor opacity shows a good correlation with the 183 GHz water vapor line opacity, and the liquid water opacity shows no correlation with the line opacity.

The results also indicate that the submillimeter opacity is less affected by liquid water than the millimeter opacity; we therefore propose to use the submillimeter opacity for the interferometric phase-correction by using the total-power outputs from submillimeter receivers for astronomical observations.

reading our manuscript. We also thank Martina C. Wiedner and our referee for helpful comments. This work is partly supported by Grant-in-Aid for Scientific Research (No. 13304015) from the Japan Society for the Promotion of Science (JSPS). This work was supported by the Inter-Research Centers Cooperative Program of the JSPS.

References

- Butler, B. J., Radford, S. J. E., Sakamoto, S., & Kohno, K. 2001, ALMA Memo, 365
- Carilli, C. L., & Holdaway, M. A. 1997, VLA Scientific Memo, 173
- Carilli, C. L., & Holdaway, M. A. 1999, *Radio Science*, 34, 817
- Carilli, C. L., Holdaway, M. A., & Sowinski, K. P. 1996, VLA Scientific Memo, 169
- Carilli, C. L., Lay, O., & Sutton, E. C. 1998, ALMA Memo, 210
- Delgado, G., Nyman, L.-Å., Otárola, A., Hills, R., & Robson, Y. 2001, ALMA Memo, 361
- Delgado, G., Otárola, A., Belitsky, V., Urbain, D., Hills, R., & Martin-Cocher, P. 1999, ALMA Memo, 271
- Delgado, G., Otárola, A., Nyman, L.-Å., Booth, R., Belitsky, V., Urbain, D., Hills, R., Robson, Y., & Martin-Cocher, P. 2000, ALMA Memo, 332
- Hills, R. E., Gibson, H., Richer, J., Smith, H., Belitsky, V., Booth, R., & Urbain, D. 2001, ALMA Memo, 352
- Hirota, T., Yamamoto, S., Sekimoto, Y., Kohno, K., Nakai, N., & Kawabe, R. 1998, PASJ, 50, 155
- Ho, P. T. P. 2000, in ASP Conf. Ser. Vol. 217, *Imaging at Radio through Submillimeter Wavelengths*, ed. J. G. Mangum & S. J. E. Radford (San Francisco: ASP), 227
- Holdaway, M. A. 1992, ALMA Memo, 84
- Holdaway, M. A., Matsushita, S., & Saito, M. 1997, ALMA Memo, 176
- Holdaway, M. A., & Owen, F. N. 1995, ALMA Memo, 126
- Hufford, G. 1991, *Intern. J. Infrared Millimeter Waves*, 12, 677
- Kohno, K., Kawabe, R., Ishiguro, M., Kato, T., Otárola, A., Booth, R., & Bronfman, L. 1995, Nobeyama Radio Observatory Technical Report, No. 42
- Lay, O. P. 1998, ALMA Memo, 209
- Liebe, H. J. 1989, *Intern. J. Infrared Millimeter Waves*, 10, 631
- Liebe, H. J., Hufford, G. A., & Cotton, M. G. 1993, in AGARD 52nd Specialists' Meeting of the Electromagnetic Wave Propagation Panel, 3-1
- Liebe, H. J., Hufford, G. A., & Manabe, T. 1991, *Intern. J. Infrared Millimeter Waves*, 12, 659
- Martin, D. H., & Pulett, E. F. 1970, *Infrared Phys.*, 10, 105
- Masson, C. R. 1994, in ASP Conf. Ser. Vol. 59, *IAU Colloquium 140, Astronomy with Millimeter and Submillimeter Wave Interferometry*, ed. M. Ishiguro & J. Welch (San Francisco: ASP), 87
- Matsuo, H., Sakamoto, A., & Matsushita, S. 1998a, PASJ, 50, 359
- Matsuo, H., Sakamoto, A., & Matsushita, S. 1998b, *Proc. SPIE*, 3357, 626
- Matsushita, S., & Matsuo, H. 2002, in ASP Conf. Ser. Vol. 266, *Astronomical Site Evaluation in the Visible and Radio Range*, ed. J. Vernin, Z. Benkhaldoun, & C. Muñoz-Tuñón (San Francisco: ASP), 180
- Matsushita, S., Matsuo, H., Pardo, J. R., & Radford, S. J. E. 1999, PASJ, 51, 603

We would like to thank Virginia Starke for carefully

- Matsushita, S., Matsuo, H., Sakamoto, A., & Pardo, J. R. 2000, Proc. SPIE, 4015, 378
- Matsushita, S., Matsuo, H., Wiedner, M. C., & Pardo, J. R. 2002, ALMA Memo, 415
- Morita, K.-I., Handa, K., Asaki, Y., Kitamura, Y., Yokogawa, S., Saito, M., Wilner, D. W., Ho, P. T. P., & Ohashi, N. 2000, in ASP Conf. Ser. Vol. 217, Imaging at Radio through Submillimeter Wavelengths, ed. J. G. Mangum & S. J. E. Radford (San Francisco: ASP), 340
- Paine, S., Blundell, R., Papa, D. C., Barrett, J. W., & Radford, S. J. E. 2000, PASP, 112, 108
- Pardo, J. R., Cernicharo, J., & Serabyn, E. 2001a, IEEE Trans. on Antennas and Propagation, 49, 1683
- Pardo, J. R., Serabyn, E., & Cernicharo, J. 2001b, J. Quant. Spec. Radiat. Transf., 68, 419
- Pardo, J. R., Wiedner, M. C., Serabyn, E., & Cernicharo, J. 2002, J. Quant. Spec. Radiat. Transf., submitted
- Radford, S. J. E. 2002, in ASP Conf. Ser. Vol. 266, Astronomical Site Evaluation in the Visible and Radio Range, ed. J. Vernin, Z. Benkhaldoun, & C. Muñoz-Tuñón (San Francisco: ASP), 148
- Radford, S. J. E., Butler, B. J., Sakamoto, S., & Kohno, K. 2001, ALMA Memo, 384
- Radford, S. J. E., & Chamberlin, R. A. 2000, ALMA Memo, 334
- Radford, S. J. E., & Holdaway, M. A. 1998, Proc. SPIE, 3357, 486
- Radford, S. J. E., Reiland, G., & Shillue, B. 1996, PASP, 108, 441
- Ray, P. S. 1972, Appl. Opt., 11, 1836
- Sakamoto, S. 2002, in ASP Conf. Ser. Vol. 266, Astronomical Site Evaluation in the Visible and Radio Range, ed. J. Vernin, Z. Benkhaldoun, & C. Muñoz-Tuñón (San Francisco: ASP), 440
- Sakamoto, S., Handa, K., Kohno, K., Nakai, N., Otárola, A., Radford, S. J. E., Butler, B., & Bronfman, L. 2000, ALMA Memo, 322
- Thompson, A. R., Moran, J. M., & Swenson, G. W., Jr. 2001, Interferometry and Synthesis in Radio Astronomy, Second Edition (New York: Wiley-Interscience)
- Warren, S. G. 1984, Appl. Opt., 23, 1206
- Wiedner, M. C., & Hills, R. E. 2000, in ASP Conf. Ser. Vol. 217, Imaging at Radio through Submillimeter Wavelengths, ed. J. G. Mangum & S. J. E. Radford (San Francisco: ASP), 327
- Wiedner, M. C., Hills, R. E., Carlstrom, J. E., & Lay, O. P. 2001, ApJ, 553, 1036
- Wiedner, M. C., Hills, R. E., & Pardo, J. R. 2002, in ASP Conf. Ser. Vol. 266, Astronomical Site Evaluation in the Visible and Radio Range, ed. J. Vernin, Z. Benkhaldoun, & C. Muñoz-Tuñón (San Francisco: ASP), 278
- Yun, M. S., & Wiedner, M. C. 1999, ALMA Memo, 252